Discovery of a novel class of AKT pleckstrin homology domain inhibitors

Daruka Mahadevan,[1] Garth Powis,[6] Eugene A. Mash,[4] Benjamin George,[2] Vijay M. Gokhale,[3] Shuxing Zhang,[6] Kishore Shakalya,[1] Lei Du-Cuny,[6] Margareta Berggren,[2] M. Ahad Ali,[4] Umasish Jana,[4] Nathan Ihle,[6] Sylvestor Moses,[5] Chloe Franklin,[6] Satya Narayan,[1] Nikhil Shirahatti,[1] and Emmanuelle J. Meuillet[2,5]

[1]College of Medicine, Arizona Cancer Center, [2]Department of Nutritional Sciences, [3]College of Pharmacy, Departments of [4]Chemistry and [5]Molecular and Cellular Biology, University of Arizona, Tucson, Arizona; and [6]Department of Experimental Therapeutics, University of Texas, M. D. Anderson Cancer Center, Houston, Texas

Abstract

AKT, a phospholipid-binding serine/threonine kinase, is a key component of the phosphoinositide 3-kinase cell survival signaling pathway that is aberrantly activated in many human cancers. Many attempts have been made to inhibit AKT; however, selectivity remains to be achieved. We have developed a novel strategy to inhibit AKT by targeting the pleckstrin homology (PH) domain. Using *in silico* library screening and interactive molecular docking, we have identified a novel class of non–lipid-based compounds that bind selectively to the PH domain of AKT, with "*in silico*" calculated K_D values ranging from 0.8 to 3.0 μmol/L. In order to determine the selectivity of these compounds for AKT, we used surface plasmon resonance to measure the binding characteristics of the compounds to the PH domains of AKT1, insulin receptor substrate-1, and 3-phosphoinositide–dependent protein kinase 1. There was excellent correlation between predicted *in silico* and measured *in vitro* K_Ds for binding to the PH domain of AKT, which were in the range 0.4 to 3.6 μmol/L. Some of the compounds exhibited PH domain–binding selectivity for AKT compared with insulin receptor substrate-1 and 3-phosphoinositide–dependent protein kinase 1. The compounds also inhibited AKT in cells, induced apoptosis, and inhibited cancer cell proliferation. *In vivo*, the lead compound failed to achieve the blood concentrations required to inhibit AKT in cells, most likely due to rapid metabolism and elimination, and did not show antitumor activity. These results show that these compounds are the first small molecules selectively targeting the PH domain of AKT. [Mol Cancer Ther 2008; 7(9):2621–32]

Introduction

The phosphoinositide 3-kinase (PI3K) pathway is critical to many aspects of cancer cell function including growth, survival, differentiation, and invasion (1, 2). PI3K phosphorylates membrane phosphatidylinositol-4,5-bisphosphate [PtdIns(4,5)P_2] to give the trisphosphate, PtdIns(3,4,5)P_3, which binds to lipid-binding domains of downstream targets, recruiting them to the membrane. PI3K signaling is activated by many growth factors and regulators of cell proliferation, whereas the tumor suppressor, phosphatase and tensin homologue deleted in chromosome 10, a dual-specificity tyrosine-threonine/phosphoinositide 3-phosphatase (3, 4), prevents the accumulation of PtdIns(3,4,5)P_3 and thus attenuates PI3K signaling (5). Constitutive activation of the pathway through mutation, amplification, and rearrangement occurs frequently in human cancer and is associated with aggressive tumor growth, increased metastasis, and resistance to therapy (1, 2). Thus, the PI3K pathway is an attractive target for cancer drug discovery that is actively being pursued by many pharmaceutical and academic groups.

The primary downstream mediator of the effects of PI3K is AKT (or protein kinase B), which binds PtdIns(3,4,5)P_3 through its NH_2-terminal pleckstrin homology (PH) domain. AKT is a 56 kDa member of the AGC serine/threonine kinase family (6). There are three known mammalian isoforms, AKT1/α, AKT2/β, and AKT3/γ, which share a high degree sequence homology in their catalytic and NH_2-terminal PH domains, but differ in the linker between the domains and the COOH-terminal extension (7). AKT1 and AKT2 are ubiquitously expressed whereas AKT3 is found predominantly in brain, heart, and kidney (8). Following PH domain membrane recruitment, AKTs are phosphorylated on conserved Thr^{308} in the activation loop and Ser^{473} in the COOH-terminal extension (9), resulting in activation of AKT kinase activity (7, 10). Phosphorylation of both residues is required for AKT activation (11). The kinase responsible for Thr^{308} phosphorylation is the constitutively active 3-phosphoinositide–dependent kinase 1 (PDK1; ref. 12) whereas Ser^{473} can be

Received 11/13/07; revised 4/14/08; accepted 5/14/08.

Grant support: RO1 CA 061015 and P30 CA 23074 from the National Cancer Institute (G. Powis) and by grant ABRC no. 9010 from the Arizona Biomedical Research Commission (E.J. Meuillet).

The costs of publication of this article were defrayed in part by the payment of page charges. This article must therefore be hereby marked *advertisement* in accordance with 18 U.S.C. Section 1734 solely to indicate this fact.

Note: D. Mahadevan and G. Powis: both authors participated equally in the work presented in this publication.

Requests for reprints: Emmanuelle J. Meuillet, Department of Nutritional Sciences, University of Arizona, 1177 East 4th Street, P.O. Box 210038, Tucson, AZ 85721-0038. Phone: 520-626-5794; Fax: 520-621-9446. E-mail: emeuillet@azcc.arizona.edu

doi:10.1158/1535-7163.MCT-07-2276

phosphorylated by integrin-linked kinase (13), the mTOR rictor complex (14), protein kinase Cε (PKCε; ref. 15) and by autophosphorylation (16). Phosphorylated AKT is independent of phospholipid activation and detaches from the plasma membrane translocating to the cytoplasm and the nucleus (17). The full activity of AKT in promoting cell survival relies on the phosphorylation of a battery of targets to either prevent the expression of death genes or to induce cell survival (18). Promoters of apoptosis that are inhibited by AKT are the forkhead transcription factor family members (FKHR, FHHRL1, and AFX; ref. 19), the proapoptotic Bcl-2 family member Bad, the apoptosis signaling kinase-1 that transduces stress signals to the c-*Jun*-NH_2-kinase and p38 mitogen-activated protein kinase pathways (20), and procaspase-9, the initiator of the caspase cell death cascade (21). Targets that AKT activates to promote cell survival are nuclear factor κB (22) and the cyclic AMP-response element binding protein (23). AKT also phosphorylates $p70^{S6kinase}$ (24) and GSK3β (25), contributing to cyclin D accumulation of cell cycle entry (26). Finally, AKT phosphorylates and activates mTOR/FRAP to increase hypoxia-inducible factor-1α, a mediator of vascular endothelial growth factor production and angiogenesis (27).

The PH domain is a ~100 to 120–amino acid modular fold found in >250 human proteins (28). PH domains have few critically conserved amino acids, but show remarkable conservation of three-dimensional structure. Crystal structures and nuclear magnetic resonance structures of several PH domains show a highly conserved three-dimensional organization, although sequence identities are only 7% to 23%. The core of each PH domain consists of a β-barrel of seven antiparallel β-strands and a COOH-terminal amphipathic α-helix. PH domains can bind to Gβγ subunits of heterotrimeric G proteins (29, 30), to certain phosphotyrosine peptides, polyproline sequences, and phosphoinositides (PtdIns). A majority of PH domain members bind PtdIns weakly and nonspecifically but a subclass of approximately 40 PH domain proteins shows high affinity for PtdIns. These PtdIns-binding PH domain proteins are important components of signal transduction pathways that regulate cancer cell growth and survival (31). PtdIns binding PH domains are classified according to their binding specificity based on conserved positively charged residues in the phosphatidylinositol phosphate (PtdInsP) binding pocket and have K_Ds in the range of 1 to 5 μmol/L (32). Group 1 PH domains specifically recognize PtdIns(3,4,5)P_3. Group 2 PH domains bind PtdIns(4,5)P_2 and also interact with other phosphoinositides, but because PtdIns(4,5)P_2 is more abundant than 3-phosphorylated phosphoinositides, PH domains in group 2 are regulated by PtdIns(4,5)P_2. Group 3 PH domains recognize PtdIns(3,4)P_2 and PtdIns(3,4,5)P_3. Group 4 PH domains have a low affinity for PtdInsP binding. Group 2 PH domains mediate the effects of PtdIns(4,5)P_2 on membrane trafficking and plasma membrane–cytoskeleton linkages, whereas group 1 and group 3 domains mediate the effects of PtdIns(3,4,5)P_3 on cell signaling pathways that regulate cell growth and survival (2). AKT has a group 3 PH domain. The crystal structure of the PH domain of AKT1 bound to the inositol head group of PtdIns(3,4,5)P_3, that is, *myo*-inositol(1,3,4,5)P_4, has been determined and the mode of binding elucidated (32). Recently, an activating mutation (Glu^{17} into Lys^{17}) has been reported in the PH domain of AKT at low frequency in human tumors (33).

There have been attempts to develop selective inhibitors of the AKT kinase ATP catalytic site as potential anticancer drugs, but a major problem has been toxicity, possibly associated with a lack of selectivity for other members of the AGC serine/threonine kinase family (34, 35). We have previously reported that a PtdIns analogue, D-3-deoxyphosphatidylinositol ether lipid (DPIEL, PX-316), binds selectively to the PH domain of AKT1, preventing the protein translocation and activation at the plasma membrane (36). In mice xenograft models of cancer, PX-316 inhibits tumor AKT and has antitumor activity (36, 37). This work was the point of departure for a cancer drug discovery effort based on the X-ray crystal structure of the AKT1 PH domain that uses *in silico* library screening, docking, structure-based design, synthesis, testing, and iterative refinement to develop novel inhibitors of AKT.

Materials and Methods

Pharmacophore Design, *In silico* Screening, and Interactive Docking

The high-resolution crystal structure of the isolated PH domain of human AKT1 in a complex with the head group of Ins(1,3,4,5)P_4 (32) was used to define a pharmacophore pocket for screening a 2,000-molecule database (National Cancer Institute) using Unity in Sybyl (version 7.2; Tripos Inc.). The pharmacophore pocket included all the residues of the AKT1 crystal structure within 5 Å of the Ins(1,3,4,5)P_4 binding site: Lys^{14}, Arg^{15}, Gly^{16}, Glu^{17}, Tyr^{18}, Ile^{19}, Lys^{20}, Thr^{21}, Arg^{23}, Pro^{24}, Arg^{25}, Lys^{39}, Pro^{51}, Leu^{52}, Asn^{53}, Asn^{54}, Phe^{55}, Gln^{79}, Ile^{84}, Glu^{85}, Arg^{86}, and Phe^{88}. The program operates by assigning attributes to various atoms on the ligand or protein binding site. The defined pharmacophore pocket was used to search virtual chemical databases and candidate compound ''hits'' were identified. The FlexX docking algorithm in Sybyl V.7.2 was used for the docking of these compounds into the AKT1 PH domain active site. FlexX produces 30 different docking orientations (poses) of the ligand within the active site. Various docking orientations were analyzed on the basis of FlexX scores, G-score, and X-score. The scores are similar to interaction energy, and the more negative the value, the better the interaction. The predicted K_D is calculated by $pK_D = 10 \exp(-Xscore)$ (38). In order to investigate the possibility of specific binding of the identified small molecules at the AKT1 PH domain using *in silico* methods, known crystal structures of the insulin receptor substrate-1 (IRS1) PH domain (IRS1, PDB:1QQG; ref. 39) and of the PDK1 PH domain (PDK1, PDB:1W1D, 1W1G; ref. 40) were also used for docking studies similar to those described above.

Synthetic Procedures

Details of the syntheses and characterizations of the compounds used herein are located in the Supplemental Data.

Expression and Purification of Recombinant PH Domains

Recombinant mouse AKT1 PH domain amino acids 1 to 111 (UBI/Millipore), human AKT1 PH domain amino acids 1 to 111 (Origene, NM005163.2), human IRS1 PH domain amino acids 12 to 133 (Invitrogen), and human PDK1 PH domain amino acids 407 to 549 (Origene, NM002613.3) were cloned by PCR into *Eco*RI/*Xho*I sites in pGEX-4T1 inducible bacterial expression plasmid (GeneStorm, InVitrogen) transformed into BL21(DE3) *Escherichia coli*.

Surface Plasmon Resonance Spectroscopy Binding Assays

All interaction analyses were done with a Biacore 2000 Control Software v3.2, and BIAevaluation v4.1 analysis software (Biacore). The PH domain GST-fusion proteins (AKT1, IRS1, and PDK1) were immobilized on a CM5 Sensorchip (Biacore BR-1000-12) using Biacore's Amine Coupling Kit (Biacore BR-1000-50) to a level of 10,000 response units. Small molecule analytes at concentrations ranging from 1/10 to 10 times the predicted K_D were injected at a high flow rate (30 μL/min). DMSO concentrations in all samples and running buffer were 1% (v/v) or less.

ELISA Competitive Binding Assay

A 96-well Maxisorb plate (Nunc) was coated with 1 μg/100 μL L-α-phosphatidylinositol(3,4,5)P_3 (Biomol). The proteins (purified GST-PH domains) were incubated with the drugs for 4 h in 0.2 mol/L of carbonate buffer (pH 9.4). The proteins mixed with increasing concentration of drugs were then added to the 96-well plate and incubated overnight at 4°C. The plate was washed four times with phosphate buffered 0.9% NaCl (PBS), blocked with 3% bovine serum albumin in PBS and 0.01% Tween for 1 h, washed again four times with PBS and mouse monoclonal anti–glutathione-*S*-transferase antibody (Pierce) in 3% bovine serum albumin (1:2,000) was added for 1 h at room temperature while shaking. The plate was washed four times with PBS and an anti-mouse IgG horseradish peroxidase–coupled antibody (dilution 1:2,000 in 3% bovine serum albumin) was added for 1 h. Following four washes with PBS, 2,2′-azinobis (3-ethylbenzothiazoline-6-sulfonic acid)-diammonium salt (Pierce) was added and the reaction was allowed to develop for 30 min. A stop solution of 1% SDS was then added and the plate was read at 405 nm in a plate reader (μQuant Bio Tek Instruments, Inc.).

Cell Culture and Compound Treatments

Human HT-29 colon cancer cells and NIH3T3 mouse fibroblast cancer cells were obtained from the American Type Culture Collection. Cells were maintained in bulk culture in DMEM supplemented with 10% heat-inactivated fetal bovine serum, 4.5 g/L of glucose, 100 units/mL of penicillin and 100 μg/mL of streptomycin in a 5% CO_2 atmosphere. Cells were passaged using 0.25% trypsin and 0.02% EDTA. Cells were confirmed to be *Mycoplasma*-free by testing them with an ELISA kit (Roche-Boehringer Mannheim). The compounds were dissolved in DMSO at a stock concentration of 10 mmol/L and then added at different concentrations directly into the culture media of the cells.

Inhibition of Phospho-Ser^{473}AKT, Phospho-Ser^{241}PDK1, and Phospho-(pan)-PKC by Western Analysis

Inhibition of the phosphorylation of AKT1, PDK1, or PKC was measured by Western blotting as described previously (36) using rabbit polyclonal antibodies to phospho-Ser^{473}-AKT, pan-phospho-PKCs, and phosho-Ser^{241}-PDK1 (New England Biolabs/Cell Signaling Technology, Inc.). Bands corresponding to phospho-AKT, phospho-PKC, or phospho-PDK1 were quantified using Eagle Eye software (Bio-Rad) and Kodak X-Omat Blue XB (NEN, Life Science Products). β-Actin was used as a loading control in all Western blots.

Cell Cytotoxicity Assay

Cell growth inhibition was determined using a microcytotoxicity assay. Cells were plated in a 96-well microtiter plate at 5,000 to 10,000 cells per well (depending on the cell doubling time) and grown for 7 days. Compounds dissolved in DMSO were added directly to the medium at various concentrations ranging from 1 to 50 μmol/L. The end point was spectrophotometric determination of the protein content of each well using 3-(4,5-dimethylthiazol-2-yl)-2,5-diphenyltetrazolium bromide. A concentration-response relationship at two or more concentration levels was used to obtain an IC_{50} for the compound.

Cell Apoptosis Assay

Apoptosis was measured as described previously in ref. (41). Briefly, HT-29 cells were grown to 70% to 75% confluency in six-well tissue culture plates. Cells were treated with the compounds for 24 h. To measure apoptosis, 10 μL of cells were mixed with an ethidium bromide and acridine orange solution (100 μg/mL each in DMEM) and visualized by immunofluorescence for morphologic changes. A minimum of 200 cells was counted and the percentage of apoptotic cells was determined.

Antitumor Activity

Approximately 1×10^7 HT-29 colon cancer cells in log phase growth were injected s.c. in 0.1 mL PBS into the flanks of female severe combined immunodeficient (*scid*) mice. When the tumors reached volumes between 100 and 170 mm^3, the mice were stratified into groups of eight animals having approximately equal mean tumor volumes and administration of compound **1** suspended in 0.2 mL of 25% DMSO in 20% pharmaceutical grade hydroxypropyl-β-cyclodextrin (Trappsol, Cyclodextrin Technologies Development) in water was started at a dose of 250 mg/kg per day p.o. daily for 5 days. The animals were weighed weekly and tumor diameters measured twice weekly at right angles (d_{short} and d_{long}) with electronic calipers and converted to volume by the formula: volume = $(d_{short})^2 \times (d_{long}) / 2$ (42). When the tumor volume reached ≥2,000 mm^3 or became necrotic, the animals were euthanized.

Pharmacokinetic Studies

Male C57Bl/6 mice were administered compound **1** i.p. or p.o. at 250 mg/kg suspended in 0.2 mL of 25% DMSO in 20% Trappsol. The mice were sacrificed at various times, blood was collected into heparinized tubes and plasma was prepared. Plasma (0.2 mL) was immediately mixed with an equal volume of 0.25 mol/L of sodium phosphate buffer (pH 4.0) and extracted for 1 h by inversion with 4 mL of ethyl acetate. After centrifugation, 3.8 mL of the organic layer was removed and evaporated under nitrogen and the residue dried on a lyophilizer. Chromatographic separation was achieved with a Waters Symmetry C-18 3.9 × 150 mm column (Waters) with a mobile phase of 0.1% trifluoroacetic acid in 60% methanol, at a flow rate of L/min with detection at 254 nm. For the assay, the sample residue was dissolved in 100 μL mobile phase and centrifuged at 15,000 × *g* for 5 min at 4°C. The limit of detection of the assay for all the compounds from 0.2 mL mouse plasma was 0.01 μg/mL.

Toxicity Studies

Compound **1** was administered at 250 mg/kg per day by oral gavage (p.o.) daily for 5 days to female *scid* mice. The mice were sacrificed 24 h after the last dose and changes in body weight from the start of the study, blood lymphocyte, neutrophil, RBC, and platelet counts, and aspartate aminotransferase and amino alanine transferase were measured.

Pharmacodynamic Studies

HT-29 colon cancer cells (1×10^7) were injected s.c. into the flanks of female *scid* mice and allowed to grow to ~300 mm^3. Mice received a single intraperitoneal dose of compound **1** (250 mg/kg) in 25% DMSO in 20% Trappsol in water. Mice were killed at various times and tumors removed and immediately frozen in liquid nitrogen. Tissues were homogenized in 50 mmol/L of HEPES buffer (pH 7.5), 50 mmol/L of NaCl, 1% NP40, and 0.25% sodium deoxycholate, and Western blotting was done using anti–phospho-Ser^{473}-AKT and anti-AKT antibodies. AKT activation was expressed as the ratio of phospho-Ser^{473}-AKT to total AKT.

Table 1. Structures and calculated properties of lead compound 1 (NSC 348900) and analogues (2–6)

Compounds	AKT1 FlexX score	AKT1 G score	AKT1 cK_D (μmol/L)	PDK1 FlexX score	PDK1 G score	PDK1 cK_D (μmol/L)	IRS1 FlexX score	IRS1 G score	IRS1 cK_D (μmol/L)
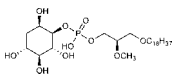	NS	NS	4.0	NS	NS	NS	NS	NS	NS
1 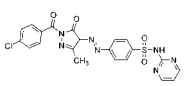	−31.0	−96.9	1.2	−17.4	−109.0	1.74	−16.0	−128.0	1.99
2 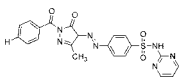	−29.6	−31.9	2.4	−17.0	−40.0	2.60	−17.1	−96.2	2.40
3 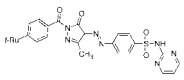	−28.2	−99.5	1.2	−17.1	−103.4	1.70	−14.8	−79.7	10.70
4 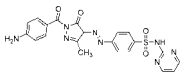	−29.1	−71.9	3.0	−17.5	−88.6	2.20	−17.9	−145.5	1.80
5 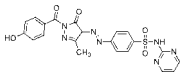	−33.0	−120.6	1.3	−20.1	−137.1	2.40	−14.6	−90.1	10.70
6 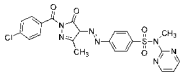	−24.3	−132.0	0.85	−21.0	−109.1	1.45	−14.5	−140.6	0.52

Abbreviation: NS, not shown.

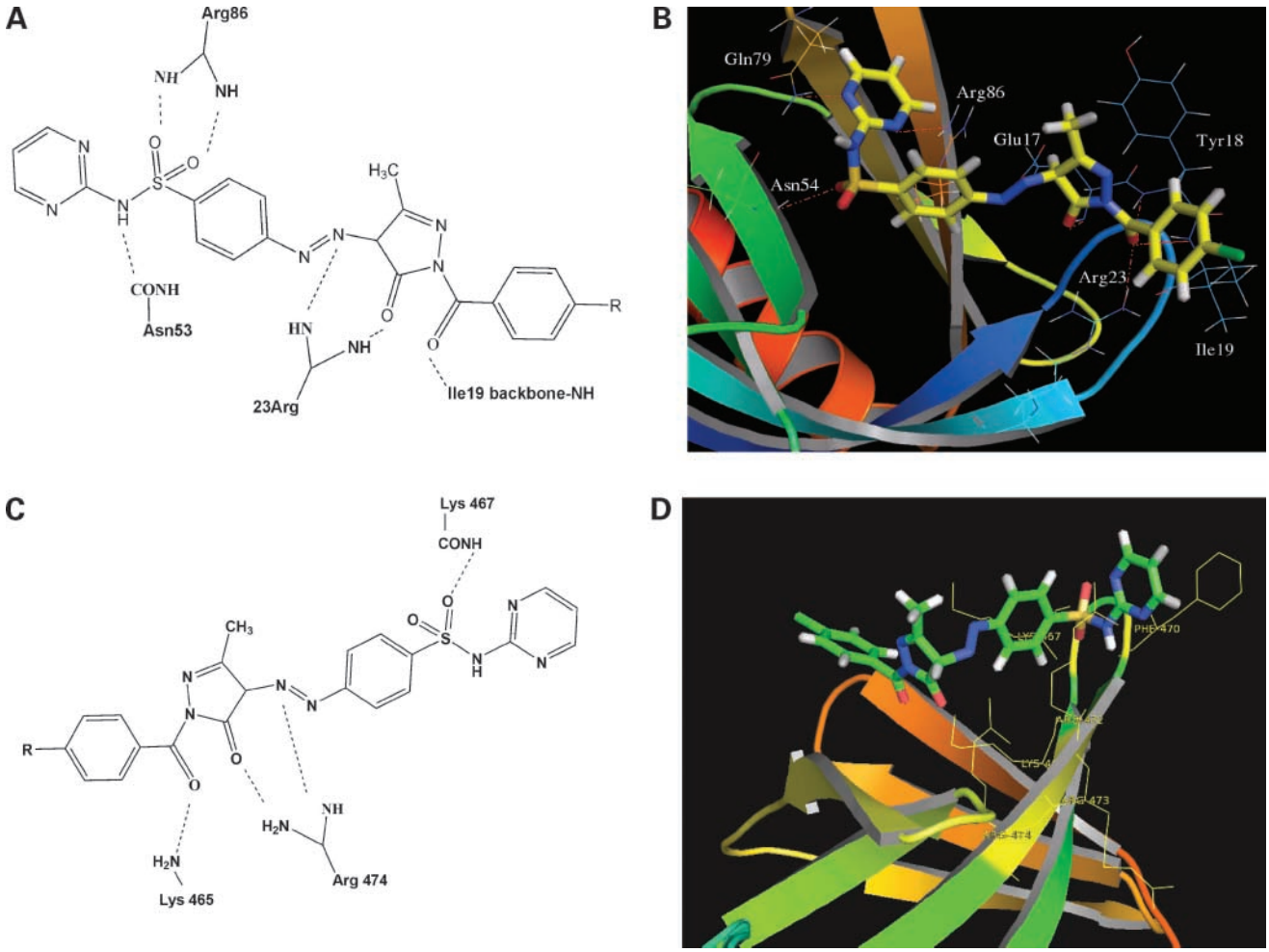

Figure 1. Interactions of compound **1** with the human AKT1 PH domain. **A,** schematic representation of the interaction of compound **1** (NSC 348900, 4-[1-(4-chlorobenzoyl)-3-methyl-5-oxo-4,5-dihydro-1H-pyrazol-4-ylazo]-*N*-pyrimidine-2-yl-benzenesulfonamide, C21H16ClN7O4S) with amino acid residues of the AKT1 PH domain (Arg^{86}, Asn^{53}, Arg^{23}, and Ile^{19}). **B,** the docking pose of compound **1** with the AKT1 PH domain. The AKT1 PH domain (*red*); residues Arg^{23}, Arg^{25}, and Arg^{86} are colored according to atom type. Compound **1** is colored according to atom type (*capped stick*). Hydrogen bonding interactions (*dotted lines*). The sulfamido group interacts with Arg^{86} through a hydrogen bonding interaction whereas similar hydrogen bonds are involved in the interaction of the diazopyrazolyl group with Arg^{23}. These two arginines are intimately involved in the interaction with the phosphate head groups of the substrate phosphoinositol-1,3,4,5-tetrakisphosphate. **C** and **D,** the binding mode of compound **1** in the binding pocket of the PH domain of PDK1 with the amino acids involved in the binding pocket (**D**). Note that compound **1** exhibits the reverse binding pose in the PDK PH domain similar to compound **2** in the PH domain of AKT1. Supplementary Fig. 1A and B show the binding mode of compound **1** in the binding pocket of the PH domain of IRS1.

Results

Discovery of Lead Molecule 1 (NSC 348900) and its Binding to the AKT1 PH Domain

$PtdIns(1,3,4,5)P_4$ and its reported interactions with the crystal structure of the AKT1 PH domain (32) provided the starting point for the identification and design of AKT1 PH domain small molecule inhibitors. A pharmacophore query search using the National Cancer Institute database led to the identification of several lead molecules. These lead molecules were docked and then ranked based on their docking scores. One of these molecules, NSC348900 (compound **1**), exhibited good FlexX score and G-score values as summarized in Table 1, and was selected as a lead for future studies. The predicted binding affinity (K_D) of compound **1** to the AKT1 PH domain was 1.2 μmol/L, which was three times better than the lipid-based compound, DPIEL with a predicted K_D of 4.0 μmol/L (Table 1). Figure 1A shows the predicted binding of compound **1** to the PH domain binding pocket of AKT1, and Fig. 1B represents hydrogen bonding interactions that occur between compound **1** and the amino acid side chains, as well as the backbone of the AKT1 PH domain binding pocket. The sulfonamido group interacts with Arg^{86} through a hydrogen bond whereas a similar hydrogen bonding interaction is involved with the diazopyrazolyl group with Arg^{23}. These two arginine residues are involved in the strong interaction with the phosphate head groups of the substrate $PtdIns(1,3,4,5)P_4$ supporting the discovery of compound **1** as an AKT1 PH domain inhibitor. Other hydrogen bonds are also established between the backbones of Ile^{19} and Asn^{53} with the sulfonamide function of the compound.

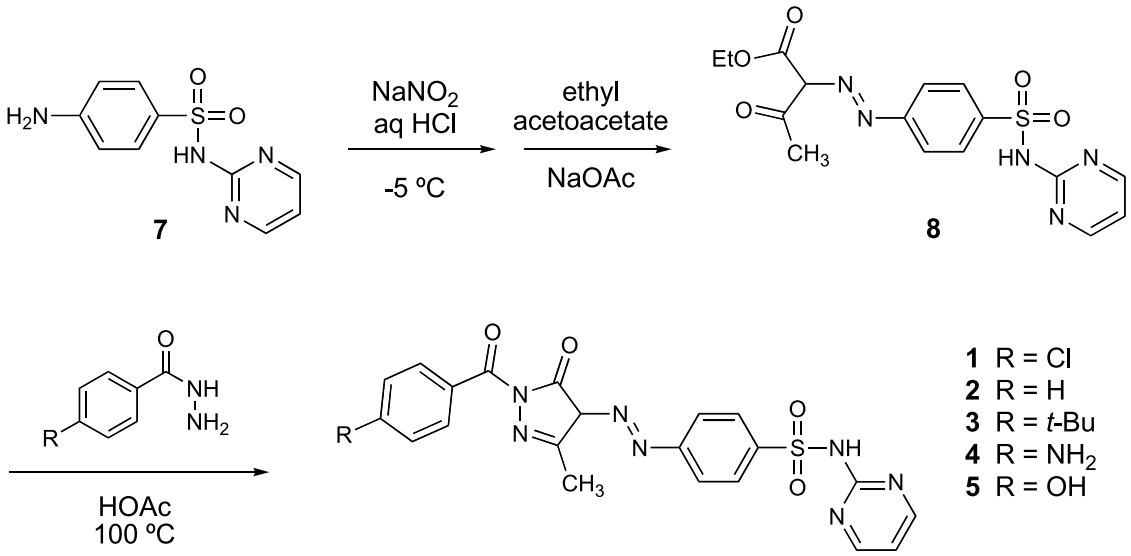

Figure 2. Synthesis of compounds **1** to **6**.

Rational Design, Chemical Synthesis, and Docking Studies of Compounds (2–6)

In order to test whether modifications of compound **1** could affect the binding properties and activity against AKT1, compound **1** and five structural analogues (compounds **2**–**6**) with varying chemical properties were synthesized (Fig. 2). Diazotization of sulfadiazine (7) with sodium nitrite under acidic conditions, followed by treatment of the diazonium salt with ethyl acetoacetate and sodium acetate, gave β-ketoester **8** in 95% yield. Condensation of compound **8** with different benzoylhydrazides in glacial acetic acid at 100°C produced NSC 348900 (1) and analogues **2** to **5** in yields ranging from 19% to 71%. Compound **6** was prepared by treatment of compound **1** with sodium hydride and methyl iodide in THF (reaction not shown). The details of these syntheses and spectroscopic data for compounds **1** to **6** and **8** are given in the Supplemental Data. The structures and docking scores for these compounds are summarized in Table 1. Analyses of the docking poses of these compounds in the PH domain of AKT1 revealed different docking orientations between compounds **1, 3**, and **5** as compared with compounds **2, 4**, and **6**. Because there are only small changes in the structures of these compounds, it is expected that these differences in docking orientations are due to limitations of the FlexX docking program (for flexible compounds). It was expected that compounds **1** to **6** would exhibit similar binding to the AKT1 PH domain.

Table 2. Sequence alignments of the PH domain of AKT

Alignment of human AKT PH domain isoforms

AA numbers	14 20 23 25 27 52 55	
AKT1 PH	MSDVAIVKEGWLH**KRGEYIK**TW**R**P**R**Y**F**LLKNDGTFIGYKERPQDVDQREAP**LNNF**SVA	58
AKT2 PH	MSDVAIVKEGWLH**KRGEYIK**TW**R**P**R**Y**F**LLKNDGTFIGYKERPQDVDQREAP**LNNF**SVA	58
AKT3 PH	MSDVTIVKEGWVQ**KRGEYIK**NW**R**P**R**Y**F**LLKTDGSFIGYKEKPQDVDLP-YP**LNNF**SVA	57
AA numbers	71 74 76	
AKT1 PH	QCQLMKTERPRP**N**TF**I**I**R**CLQWTTVIERTFHVETPEEREEWTTAIQTVADGL	110
AKT2 PH	QCQLMKTERPRP**N**TF**I**I**R**CLQWTTVIERTFHVETPEEREEWTTAIQTVADGL	110
AKT3 PH	KCQLMKTERPKP**N**TF**I**I**R**CLQWTTVIERTFHVDTPEEREEWTEAIQAVADRL	109

Alignment of human (h) and mouse (m) AKT PH domains

AA numbers	14 20 23 25 27 52 55	
hAKT PH	MSDVAIVKEGWLH**KRGEYIK**TW**R**P**R**Y**F**LLKNDGTFIGYKERPQDVDQREAPL**NNF**SVAQC	
mAKT PH	MNDVAIVKEGWLH**KRGEYIK**TW**R**P**R**Y**F**LLKNDGTFIGYKERPQDVDQRESPL**NNF**SVAQC	
AA numbers	71 74 76	
hAKT PH	QLMKTERPRP**N**TF**I**I**R**CLQWTTVIERTFHVETPEEREEWTTAIQTVADGL	110
mAKT PH	QLMKTERPRP**N**TF**I**I**R**CLQWTTVIERTFHVETPEEREEWATAIQTVADGL	110

NOTE: The PH domain binding residues are shown underlined in the sequence alignment above obtained using CLUSTAL W (1.82) multiple sequence alignment.

Table 3. Selectivity for other PH domains

Compounds	AKT1 PH mK_D (μmol/L)	IRS1 PH mK_D (μmol/L)	PDK1 PH mK_D (μmol/L)
PtdIns(3,4,5)P_3	3.08 ± 0.49	ND	ND
DPIEL	5.04 ± 0.48	31.56 ± 8.49	NB
1	0.37 ± 0.04	0.39 ± 0.01	31.28 ± 9.54
2	3.66 ± 0.03	NB	0.17 ± 0.10
3	1.37 ± 0.25	NB	3.57 ± 0.96
4	0.51 ± 0.06	0.14 ± 0.02	NB
5	1.35 ± 0.02	1.74 ± 0.41	0.42 ± 0.17
6	1.62 ± 0.02	NB	0.98 ± 0.48

NOTE: Binding affinities were measured by surface plasmon resonance spectroscopy as described in Materials and Methods and are referred to as mK_D (μmol/L) for measured.
Abbreviations: NB, no measurable binding; ND, not determined.

The sequence alignments of critical binding residues in the PH domains of the three human isoforms, AKT1, AKT2, and AKT3 are identical (Table 2), and thus indicate that compounds **1** to **6** should bind equally well to the three isoforms of AKT. K_Ds were also calculated for the binding of the compounds **1** to **6** to the PH domain of PDK1 and were found to be very similar to those for AKT1 (Table 1). The calculated K_Ds for the binding of compounds **1** to **6** to the PH domain of IRS1 showed greater variability with compound **6** having the greatest affinity and compounds **3** and **5** having more than an order of magnitude lower affinity. Figure 1C and D represent the binding mode of compound **1** in the binding pocket of the PH domain of PDK1 (Supplemental Fig. S1A and B show the binding mode of compound **1** in the binding pocket of the PH domain of IRS1). Compound **1** exhibits the reverse docking mode in IRS1 PH and PDK1 PH domains similar to compound **2** in the PH domain of AKT1.

Measured Binding Affinity of Compound 1 and Analogue Compounds 2 to 6

In order to validate the *in silico* data and the docking studies, binding assays using the Biacore SPR biosensor and an ELISA competitive binding assay were used to measure the binding affinity (K_D) of the compounds to all

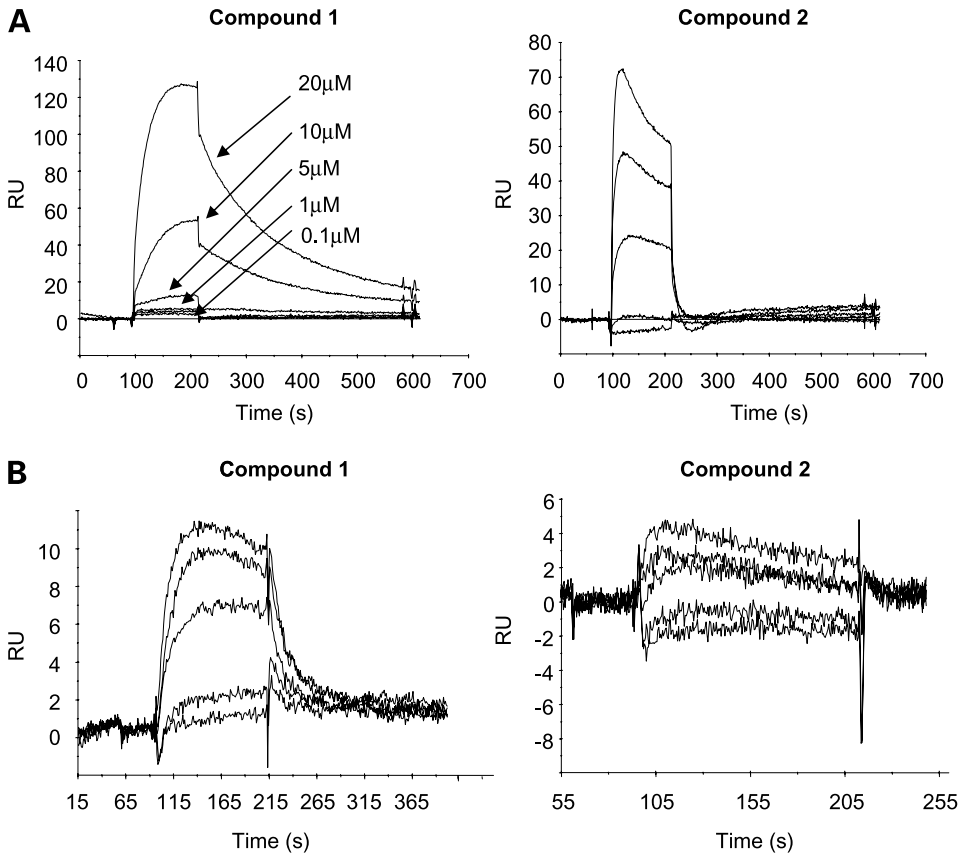

Figure 3. Binding of the compounds (**1 – 2**) to the PH domain of AKT1 and IRS1. The proteins were immobilized on a CM5 Sensorchip as described in Materials and Methods. The drugs were injected over the surface at the indicated concentrations and binding to the proteins was measured by surface plasmon resonance. **A,** the binding curves of compound **1** (*left*) and compound **2** (*right*) to the PH domain of AKT. **B,** the binding curves of compound **1** (*left*) and compound **2** (*right*) binding to the PH domain of IRS1. Overlay plot of typical sensorgrams obtained with increasing concentrations of compound **1** or **2** (*arrows*; **A**).

three PH domains. Table 3 summarizes the results obtained from the Biacore SPR measurements, which correlated well with the predicted K_D values for the compounds for each PH domain. Representative saturation curves as well dose-response curves are shown in Fig. 3 for compounds **1** and **2** to the PH domain of AKT1 (A) and to the PH domain of IRS-1 (B). Compounds **1** and **2**, which modeling suggests binds in a reverse binding pose in the PH domain binding pockets of the three different PH domains, also exhibited very different biosensor binding curves. An ELISA competitive binding assay was conducted using the PH domains of AKT1 and IRS1 with compounds **1** (Fig. 4A) and **2** (Fig. 4B). The ELISA gave binding IC_{50}s with AKT1 for compound **1** and **2** of 0.08 μmol/L, and with IRS1 for compound **1** of 1.0 μmol/L, and compound **2** of >100 μmol/L. These IC_{50}s were similar to ones obtained using Biacore.

Finally, consistent with the docking studies, compounds **1, 4**, and **5** exhibited low K_D, whereas compounds **2, 3**, and **6** do not show any binding to the IRS-1 PH domain as measured by Biacore SPR. However, compounds **4** and **6** did not bind the PH domain of PDK1, whereas the calculated K_D was predicted to be 2.2 and 1.4, respectively. Taken together, these data suggest that the structural modifications in compound **1** have altered the binding positions of the compounds in the AKT1 PH domain as well as modified their specificity against IRS1 or PDK1 PH domains. Overall, the predicted binding affinities correlated well with measured binding constants for AKT1 and PDK1 PH domains but were less accurate for the IRS-1 PH domain.

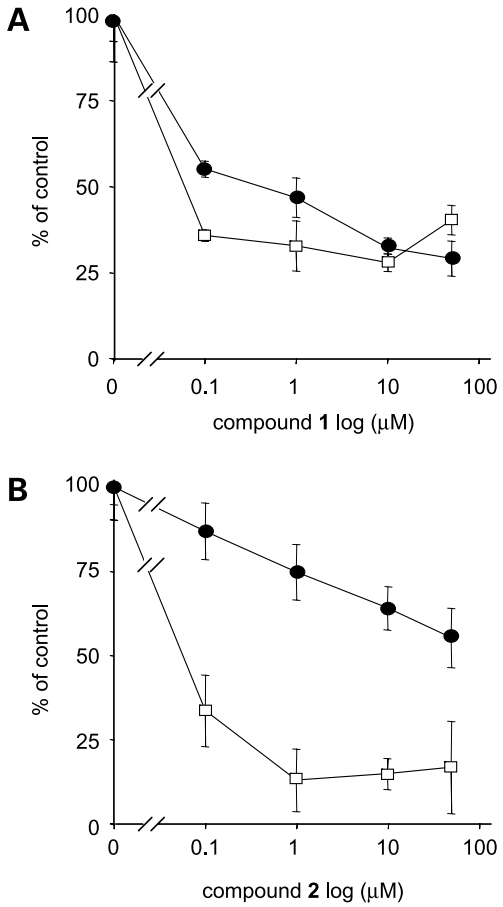

Figure 4. ELISA competitive binding assay. Competition binding curves for compounds **1** (**A**) and **2** (**B**), respectively, to the (□) AKT PH domain and (●) IRS1 PH domain. *Points,* mean of three determinations; *bars,* SD (**, $P < 0.05$). Compound **1** binds the PH domains of AKT1 and IRS1 in a similar manner. Compound **2** binds only the PH domain of AKT1.

Biological Activities of Compounds 1 to 6 in Cancer Cells

Next, the ability of the compounds (**1**–**6**) to inhibit phospho-Ser^{473}AKT was measured in cancer cells (Table 4). All compounds, except compound **3**, the most lipophilic of the compounds, inhibited phospho-Ser^{473}AKT with IC_{50}s ranging from 2-fold to 10-fold higher than required to bind to the AKT1 PH domain. Figure 5 shows typical Western blots obtained for the compounds in HT-29 colon cancer cells (A) and with concentration responses for compound **1** (C) and compound **2** (D). AKT phosphorylation was decreased in a concentration-dependent manner by increasing amounts of compounds **1** and **2** (C and D, respectively). The phosphorylation of PDK and downstream target PKC were also decreased upon treatment of the cells with compound **1** (C). IRS1 phosphorylation could not be detected in these cells (data not shown). Compound **2** mainly inhibited Akt phosphorylation with no effect on the phosphorylation of PDK or PKC. Cytotoxicity for compounds **1, 2**, and **3** was in the same range for inhibition of cell phospho-Ser^{473}AKT whereas compounds **4** and **5** showed no cytotoxicity (Table 4). Apoptosis was also measured and correlated well with Akt inhibition in HT-29 (Fig. 5B). Compounds **2** and **6** induced 60% to 50% apoptosis at 20 μmol/L and both compounds inhibited AKT as well as downstream targets such as GSK3 phosphorylation (A).

In vivo Effects of the AKT1 PH Domain Inhibitor

Absorption, metabolism, distribution, and elimination properties of compound **1** (NSC 348900) were predicted using the QikProp software (Schrodinger, Inc.). Metabolism predictions suggested that the azo-(—N = N—) linkage in the compounds might be susceptible to metabolic reduction. The stability of the compounds in cell culture conditions was measured and showed relatively rapid breakdown for compounds 1, 2, 3, and 5 with half-lives of 1 to 2 h, whereas compound **4** showed no breakdown over the time period studied (Table 4). Compound **6** was too insoluble to obtain any data.

Compound **1** was chosen for *in vivo* evaluation as the most promising and potent AKT PH domain binding compound. The compound is very insoluble and thus was administered as a slurry in 25% DMSO 20% Trappsol. Preliminary studies showed no toxicity as a single dose up to 250 mg/kg which was the maximum dose that could practically be administered i.p. Five daily doses at 250 mg/kg i.p. gave a moderate neutropenia but no other sign of toxicity with no change in body weight, blood lymphocyte, RBC and platelet count, or aspartate amino-

Table 4. Biological properties of compound 1 and analogues

Compound	AKT inhibition (IC_{50} μmol/L)		Cytotoxicity (IC_{50} μmol/L)	Log *P*	Metabolic half-life (min)	Solubility (μmol/L)	Permeability (nm/s)	
	NIH3T3	HT-29					Caco2	MDCK
1	4	13	24	2.1	62	17.9	90	91
2	11	20	14	1.9	62	28.3	83	34
3	>20	>20	25	3.2	91	28.6	95	39
4	ND	>20	NI	1.2	>480	12.9	23	8
5	5	>20	NI	1.5	138	13.1	185	200
6	3	5	ND	1.9	ND	<0.1	14	5

NOTE: For each of the analogues, phospho-Ser^{473} AKT inhibition was measured in either mouse NIH3T3 or human HT-29 colon cancer cells. Cytotoxicity was measured in HT-29 cells. Metabolic stability was measured by incubating with HT-29 cells at the maximum concentration in DMEM at 37°C. The apparent permeability (nm/s) in Caco-2 and MDCK cells was obtained using the QikProp software (Schrodinger Inc.). Values ranged between <25 for poor and >500 for great permeability.

Abbreviations: NI, not inhibitory for IC_{50} >100 μmol/L; ND, not determined.

transferase or amino alanine transferase. Pharmacokinetic studies of a single dose of compound **1** of 250 mg/kg showed a peak concentration of 1.4 μmol/L for i.p. administration and 0.6 μmol/L for p.o. administration with a relative area under the plasma concentration time curve for p.o. compared with i.p. administration of 53.0% (Fig. 6A). The failure to achieve high plasma concentrations and the relatively rapid elimination of parent compound over 24 hours despite the very large doses given, suggest rapid metabolism or elimination. Concentrations required to inhibit AKT based on the cell studies of ~4 to 13 μmol/L were not achieved. Antitumor studies showed no activity of compound **1** given p.o. daily for 5 days at 250 mg/kg against HT29 colon cancer (Fig. 6B). There was a small inhibition of tumor phospho-Ser^{473}AKT 4 hours after a single dose of compound **1** but no inhibition at 24 hours (Fig. 6C). Unexpectedly, at 24 hours, there was a significant decrease in total AKT compared with the actin loading control. Taken together, the results suggest that the limited solubility of compound **1**, and metabolism or elimination, limit the plasma concentrations that can be achieved, thus, preventing effective inhibition of AKT and possible antitumor activity. Despite no clear antitumor activity, given that compound **1** can inhibit AKT phosphorylation, it can be hypothesized that tumor cells may be sensitized for and be susceptible to chemotherapy and/or radiation treatment.

Discussion

Targeting AKT for the treatment of cancer has remained challenging (reviewed in ref. 43). Several ATP site inhibitors of Akt are relatively toxic compounds, probably because other serine/threonine kinases are being inhibited (43). On the other hand, the lipid-based PH domain inhibitors such DPIEL and perifosine are relatively nontoxic compounds (37, 44). Thus, we believe that inhibiting the PH domain could offer a better therapeutic approach than the ATP site inhibitors. We and others have developed lipid-based inhibitors of AKT designed to bind the PH domain of AKT (36, 37, 45, 46). These compounds were shown to inhibit AKT translocation, phosphorylation, and to induce apoptosis in cancer cells (36, 47). However, the potency and lack of oral bioavailability are the main problems associated in the further development of this type of compound. Thus, we sought to develop novel chemical small molecules capable of binding the PH domain of AKT. In this study, we identified a non–lipid-based compound (NSC 348900) and several analogue compounds have been synthesized and tested *in vitro* and *in vivo* for their ability to bind the PH domain of AKT. Some of the compounds exhibited selectivity for the PH domain of AKT compared with IRS1 and PDK1 PH domains. These compounds showed some activity in the cell models but did not show strong antitumor activity in the *in vivo* models of cancer.

The docking models developed for AKT PH domain inhibition used three different docking scores—FlexX score, G-score, and X-score to evaluate the interaction of the compounds with the targeted protein. These models were successful in predicting K_D values for binding to the AKT1 PH domain for the different compounds compared with K_Ds measured using surface plasmon resonance technology. However, there were apparent inconsistencies in the docking model of compounds **1** to **6** in the PH domain of IRS1. This might be because the stability and the specificity of IRS1 PH domain binding to phosphoinositides is different compared with the PH domain of AKT. Competitive binding of phosphoinositides to IRS1 PH domain indicate that phosphorylation at the 5-position on the *myo*-inositol ring contributes to the affinity and specificity because PtdIns(3,4,5)P_3 and PtdIns(4,5)P_2 bind to the PH domain with greater affinity than PtdIns(3,4)P_2 and PtdIns(4)P. Binding complexes of phosphoinositides to isolated PH domains have been reported to be unstable (39, 40). Second, and more importantly, the docking orientation of the compounds may explain the differences between modeling and *in vitro* results using surface plasmon resonance measurements. As shown in Fig. 1, the docking orientations of compound **1** in AKT1 PH

domain and IRS1 PH domain are different (flipped). In case of the AKT1 PH domain, the chlorophenyl ring (R group) is exposed to the water pocket and does not interact extensively with the PH domain residues. In case of the IRS1 PH domain, the R group interacts with the active site residues of the PH domain pocket. Hence, the changes in the R substituents showed a significant effect on binding to IRS-1 PH domain. We show for the first time that some of the compounds were also capable of binding to the PH domain of PDK1. Increasing the bioavailability of such compounds may lead to the inhibition of AKT activity. A recent study has reported that PDK1 binds in a complex with AKT, potentially via the PH domain of Akt, regulating the kinase's activation (48). This may interfere with the ability of the compounds to bind to the PH domain of AKT. Finally, although these compounds were identified and designed to specifically bind the PH domain of AKT, one cannot rule out their possible effects on other kinases involved in the pathway.

Metabolism predictions on compound **1** suggested that the azo-(—N = N—) linkage is metabolically unstable. These results may explain antitumor studies of the most specific and potent of the compounds (compound **1**), which showed no activity against HT-29 colon cancer xenografts in mice. There was no inhibition of tumor phospho-Ser^{473} AKT, most likely due to a failure to achieve sufficient plasma concentrations because of rapid metabolism or elimination despite the lack of toxicity and the large doses that could be administered. Taken together, the results suggest that inadequate solubility and pharmacokinetic properties may limit the ability of the azo sulfonamides developed in this study to inhibit AKT *in vivo*. We have,

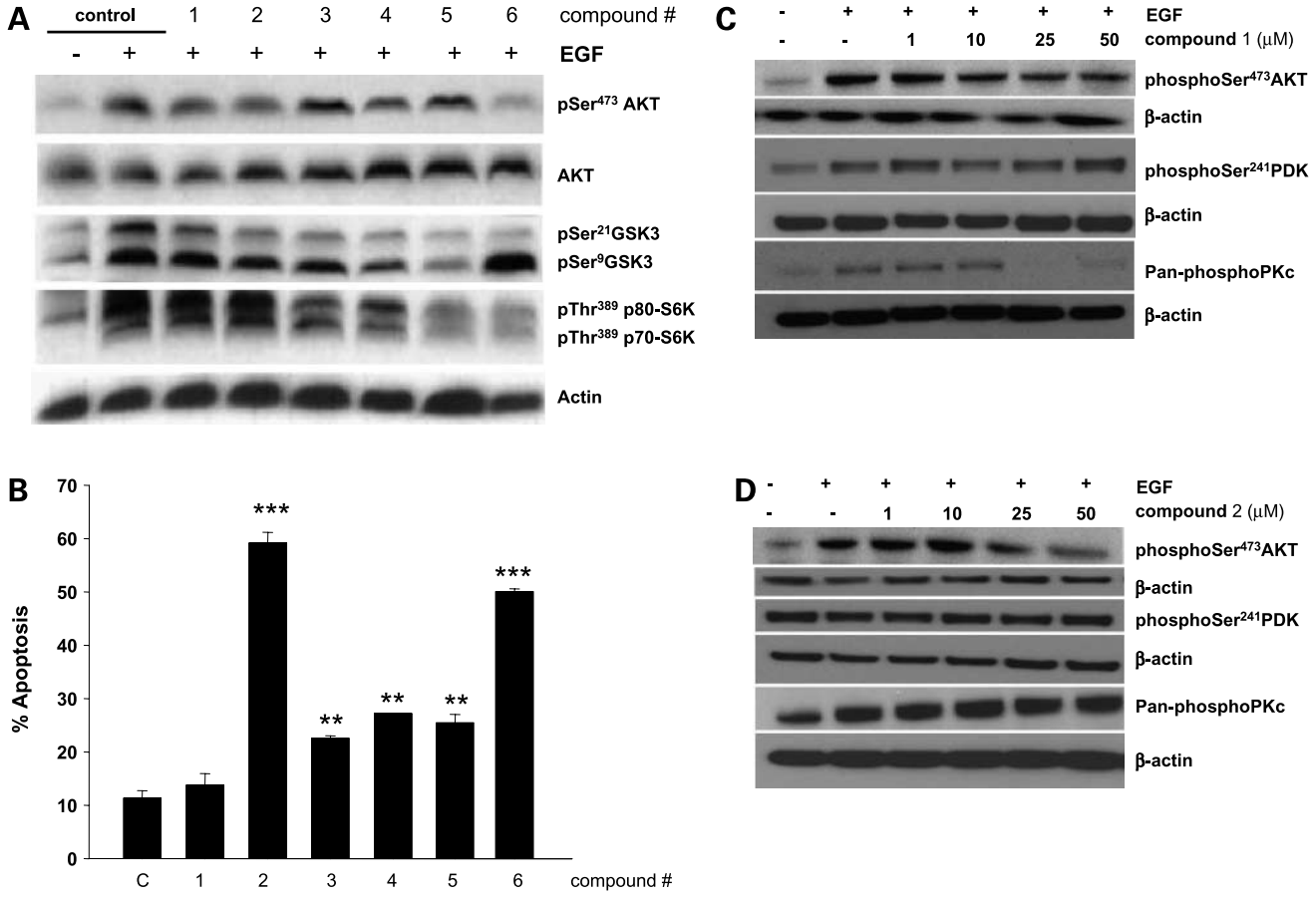

Figure 5. Inhibition of AKT in cancer cells. **A,** HT-29 colon cancer cells were treated with compounds **1** to **6**, at 20 μmol/L for 2 h and stimulated with 50 ng/nL of epidermal growth factor for 30 min. Akt activity was measured by Western blotting using anti–phospho-Ser^{437} AKT antibody. All other downstream targets of AKT were also detected by Western blotting using specific anti–phospho-antibodies. β-Actin was used as a loading control. Note that compounds **2** and **6** inhibit AKT phosphorylation and downstream GSK3 phosphorylation. **B,** apoptosis measured as described in Materials and Methods. Note that both compounds **2** and **6** at 20 μmol/L induce significant apoptosis significantly as compared with controls. *Columns,* mean of three determinations; *bars,* SD (**, $P < 0.05$ and ***, $P < 0.001$). Compound **1** (**C**) or its analogue compound **2** (**D**) were also tested at the concentrations shown for 2 h, and in HT-29 cells, stimulated with 50 ng/nL of epidermal growth factor for 30 min. Akt activity was measured by Western blotting using anti–phospho-Ser^{437} AKT antibody, PDK activity by anti–phospho-Ser^{241} PDK antibody as well as downstream target PKC using pan–phospho-PKC antibodies. β-Actin was used as a loading control.

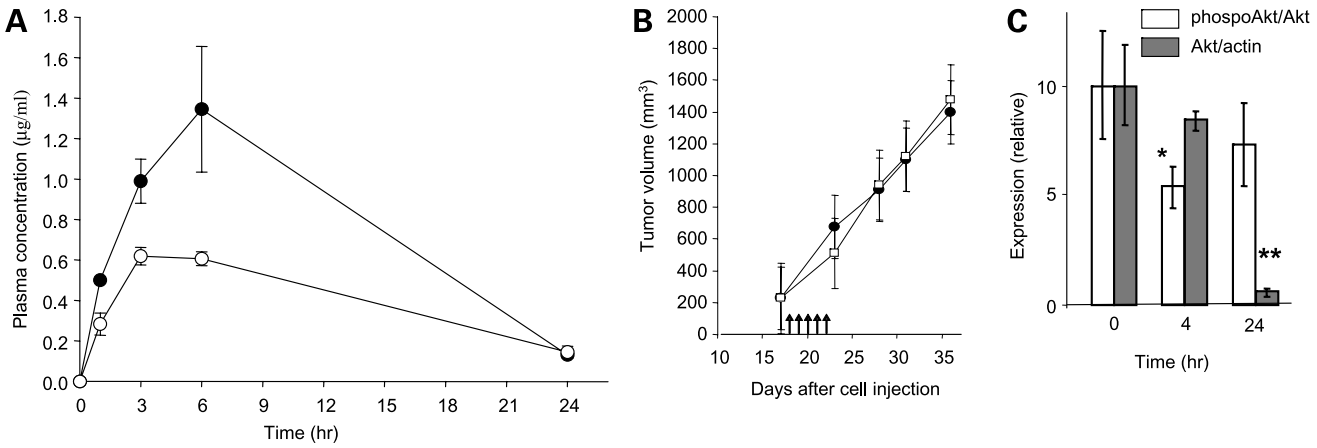

Figure 6. *In vivo* activity of compound **1**. **A,** pharmacokinetics of compound **1** in mice. Female *scid* mice were administered compound **1** at a dose of 250 mg/kg either (●) i.p. or (○) p.o. by oral gavage and plasma concentrations measured. *Points,* means of three mice; *bars,* SE. **B,** antitumor activity in female *scid* mice with HT-29 colon cancer xenografts treated p.o. daily for 5 d (*arrows*) with (●) vehicle alone or (□) compound **1** at 250 mg/kg daily. *Points,* means of 10 mice; *bars,* SE. **C,** Effect on tumor phospho-AKT in female *scid* mice with HT-29 colon cancer xenografts treated p.o. with (*open columns*) vehicle alone or (*filled columns*) compound **1** at 250 mg/kg. Tumors were removed at various times for Western blotting. *Columns,* mean of four mice; *bars,* SE (*, $P < 0.05$; **, $P < 0.01$).

however, previously reported that the lipid compound DPIEL (PX-316), which binds to the PH domain of AKT1, when administered to mice inhibits tumor AKT activity and exhibits moderate antitumor activity (36, 37). This was observed despite the fact that DPIEL does not have the properties of a good drug molecule. Thus, whereas AKT PH domain inhibitors can work *in vivo* and exhibit antitumor activity, the design of more metabolically stable and soluble analogues with improved drug-like properties should improve the activity of this new class of compounds.

In summary, using *in silico* library screening and interactive molecular docking, we have identified a novel class of non–lipid-based compounds that bind selectively to the PH domain of AKT. Calculated K_Ds compared favorably with K_Ds measured using surface plasmon resonance. Some of the compounds exhibited PH domain binding selectivity for AKT compared with IRS1 and PDK1. The compounds inhibited AKT in cells and inhibited cancer cell proliferation. The lead compound failed to achieve blood concentrations required to inhibit AKT in cells, most likely due to rapid metabolism and elimination, and did not show antitumor activity.

Disclosure of Potential Conflicts of Interest

No potential conflicts of interest were disclosed.

Acknowledgments

We thank Dr. Hariprasad Vankayalapati for input into pharmacophore design and screening of *in silico* databases.

References

1. Workman P, Clarke PA, Guillard S, Raynaud FI. Drugging the PI3 kinome. Nat Biotechnol 2006;24:794 – 6.

2. Hennessy BT, Smith DL, Ram PT, Lu Yling Y, Mills GB. Exploiting the PI3K/AKT pathway for cancer drug discovery. Nat Rev Drug Discov 2004; 4:988 – 1004.

3. Maehama T, Dixon JE. The tumor suppressor, PTEN/MMAC1, dephosphorylates the lipid second messenger, phosphatidylinositol 3,4,5-trisphosphate. J Biol Chem 1998;273:13375 – 8.

4. Wu X, Senechal K, Neshat MS, Whang YE, Sawyers CL. The PTEN/MMAC1 tumor suppressor phosphatase functions as a negative regulator of the phosphoinositide 3-kinase/AKT pathway. Proc Natl Acad Sci U S A 1998;95:15587 – 91.

5. Cantley L, Neel BG. New insights into tumor suppression: PTEN suppress tumor formation by restraining the phosphoinositide 3-kinase/AKT pathways. Proc Natl Acad Sci U S A 1999;96:4240 – 5.

6. Marte BM, Downward J. PKB/AKT: connecting phosphoinositide 3-kinase to cell survival and beyond. Trends Biochem Sci 1997;22:355 – 8.

7. Coffer PJ, Jin J, Woodgett JR. Protein kinase B (c-AKT): a multifunctional mediator of phosphatidylinositol 3-kinase activation. Biochem J 1998;335:1 – 13.

8. Nakatani K, Thompson DA, Barthel A, et al. Up-regulation of AKT3 in estrogen receptor-deficient breast cancers and androgen-independent prostate cancer lines. J Biol Chem 1999;274:21525 – 32.

9. Alessi DR, Cohen P. Mechanism of activation and function of protein kinase B. Curr Opin Genet Dev 1998;8:55 – 62.

10. Scheid MP, Woodgett JR. Unravelling the activation mechanisms of protein kinase B/AKT. FEBS Lett 2003;546:108 – 12.

11. Scheid MP, Woodgett JR. PKb/AKT: functional insights from genetic models. Nat Rev Mol Cell Biol 2001;2:760 – 8.

12. Alessi DR, James SR, Downes CP, et al. Characterization of a 3-phosphoinositide-dependent protein kinase which phosphorylates and activates protein kinase Bα. Curr Biol 1997;7:261 – 9.

13. Delcommenne M, Tan C, Gray V, et al. Phosphoinositide-3-OH kinase-dependent regulation of glycogen synthase kinase 3 and protein kinase B/AKT by the integrin-linked kinase. Proc Natl Acad Sci U S A 1998;95: 11211 – 6.

14. Sarbassov dos D, Guertin DA, Ali SM, Sabatini DM. Phosphorylation and regulation of PKB by the mTor-rictor complex. Science 2005;307: 1098 – 101.

15. Kawakami Y, Nishimoto H, Kitaura J, et al. Protein kinase Cβll regulates AKT phosphorylation on Ser-473 in a cell type and stimulus specific fashion. J Biol Chem 2004;279:47720 – 5.

16. Yang ZZ, Tschopp O, Hemmings-Mieszczak M, et al. Protein kinase Bα/AKT1 regulates placental growth and fetal growth. J Biol Chem 2003; 278:32124 – 31.

17. Meier R, Alessi DR, Cron P, Andjelkovic M, Hemmings BA. Mitogenic activation, phosphorylation, and nuclear translocation of protein kinase Bβ. J Biol Chem 1997;272:30491 – 7.

18. Nicholson KM, Anderson NG. The protein kinase B/AKT signaling pathway in human malignancy. Cell Signal 2002;14:381 – 95.

19. Datta SR, Dudek H, Tao X, et al. AKT phosphorylation of BAD couples survival signals to the cell-intrinsic death machinery. Cell 1997;91:231 – 41.

20. Kim AH, Khursigara G, Sun X, Franke TF, Chao MV. AKT phosphorylates and negatively regulates apoptosis signal-regulating kinase 1. Mol Cell Biol 2001;21:893 – 901.

21. Cardone MH, Roy N, Stennicke HR, et al. Regulation of cell death protease caspase-9 by phosphorylation. Science 1998;282:1318 – 21.

22. Ozes ON, Mayo LD, Gustin JA, et al. NF-κB activation by tumour necrosis factor requires the AKT serine-threonine kinase. Nature 1999; 401:82 – 5.

23. Du K, Montminy M. CREB is a regulatory target for the protein kinase AKT/PKB. J Biol Chem 1998;273:32377 – 9.

24. Chung J, Grammer TC, Lemon KP, Kazlauskas A, Blenis J. PDGF- and insulin-dependent pp70S6k activation mediated by phosphatidylinositol-3-OH kinase. Nature 1994;370:71 – 5.

25. van Weeren PC, de Bruyn KM, de Vries-Smits AM, Van Lint J, Burgering BM. Essential role for protein kinase B(PKB) in insulin-induced glycogen synthase kinase 3 inactivation: characterization of dominant-negative mutant of PKB. J Biol Chem 1998;273:13150 – 6.

26. Kerbel RS, Yu J, Tran J, et al. Possible mechanisms of acquired resistance to anti-angiangenic drugs: implications for the use of combination therapy approaches. Cancer Metast Rev 2001;20:79 – 86.

27. Zhong H, Chiles K, Feldser D, et al. Modulation of hypoxia-inducible factor 1α expression by the epidermal growth factor/phosphatidylinositol-3 kinase/PTEN/AKT/FRAP pathway in human prostate cancer cells: implications for tumor angiogenesis and therapeutics. Cancer Res 2000; 60:1541 – 5.

28. Rebecchi MJ, Scarlata S. Pleckstrin homology domains: a common fold with diverse functions. Annu Rev Biophys Biomol Struct 1998;27: 503 – 28.

29. Touhara K, Inglese J, Pitcher JA, Shaw G, Lefkowitz RJ. Binding of G protein βγ-subunits to pleckstrin homology domains. J Biol Chem 1994; 269:10217 – 20.

30. Mahadevan D, Thank N, Singh J, et al. Structural studies of the PH domains of Dbl, SOs1, IRS-1 and βARK1 and their differential binding to Gβγ subunits. Biochemistry 1995;34:9111 – 7.

31. Czech MP. Pip2 and pip3: complex roles at the cell surface. Cell 2000;100:603 – 6.

32. Thomas CC, Deak M, Alessi DR, van Aalten DM. High-resolution structure of the pleckstrin homology domain of protein kinase b/AKT bound to phosphatidylinositol (3,4,5)-trisphosphate. Curr Biol 2002;12:1256 – 62.

33. Carpten JD, Faber AL, Horn C, et al. A transforming mutation in the pleckstrin homology domain of AKT1 in cancer. Nature 2007;448:439 – 44.

34. Feldman R, Wu J, Polokoff M, et al. Novel small molecule inhibitors of 3′-phosphoinositide-dependent kinsase1 (PDK-1). Eur J Cancer 2004;2:77.

35. Giranda V, Luo Y, Li Q, et al. Novel ATP-competitive AKT inhibitors slow the progression of tumors *in vivo*. Eur J Cancer 2004;2:77.

36. Meuillet EJ, Mahadevan D, Vankayalapati H, et al. Specific inhibition of the AKT1 pleckstrin homology domain by D-3-deoxy-phosphatidyl-myo-inositol analogs. Mol Cancer Ther 2003;2:389 – 99.

37. Meuillet EJ, Ihle N, Baker AF, et al. *In vivo* molecular pharmacology and antitumor activity of the targeted AKT inhibitor PX-316. Oncol Res 2004;14:513 – 27.

38. Wang R, Lai L, Wang S. Further development and validation of empirical scoring functions for structure-based binding affinity prediction. J Comput Aided Mol Des 2002;16:11 – 26.

39. Dhe-Paganon S, Ottinger EA, Nolte RT, Eck MJ, Shoelson SE. Crystal structure of the pleckstrin homology-phosphotyrosine binding (PH-PTB) targeting region of insulin receptor substrate 1. Proc Natl Acad Sci U S A 1999;96:8378 – 83.

40. Komander D, Fairservice A, Deak M, et al. Structural insights into the regulation of Pdk1 by phosphoinositides and inositol phosphates. EMBO J 2004;23:3918 – 28.

41. Powell AA, LaRue JM, Batta AK, Martinez JD. Bile acid hydrophobicity is correlated with induction of apoptosis and/or growth arrest in HCT116 cells. Biochem J 2001;356:481 – 6.

42. Paine-Murrieta GD, Taylor CW, Curtis RA, et al. Human tumor models in the severe combined immune deficient *scid* mouse. Cancer Chemother Pharmacol 1997;40:209 – 14.

43. Kumar CC, Madison V. AKT crystal structure and AKT-specific inhibitors. Oncogene 2005;24:7493 – 501.

44. Catley L, Hideshima T, Chauhan D, et al. Alkyl phospholipids perifosine induces myeloid hyperplasia in a murin myeloma model. Exp Hematol 2007;35:1038 – 46.

45. Kim D, Cheng GZ, Lindsley CW, Yang H, Cheng JQ. Targeting the phosphatidylinositol-3 kinase/Akt pathway for the treatment of cancer. Curr Opin Investig Drugs 2005;6:1250 – 8.

46. Gills J, Holbeck S, Hollingshead M, et al. Spectrum of activity and molecular correlates of response to phosphatidylinositol ether lipid analogues, novel lipid-based inhibitors of Akt. Mol Cancer Ther 2006;5: 713 – 22.

47. Castillo SS, Brognard J, Petukhov PA, et al. Preferential inhibition of Akt and killing of Akt-dependent cancer cells by rationally designed phophatidylinositol ether lipid analogues. Cancer Res 2004;64:2792 – 92.

48. Calleja V, Alcor D, Laguerre M, et al. Intramolecular and intermolecular interactions of protein kinase B define its activation *in vivo*. PLoS Biol 2007;5:e95.

Molecular Cancer Therapeutics

Discovery of a novel class of AKT pleckstrin homology domain inhibitors

Daruka Mahadevan, Garth Powis, Eugene A. Mash, et al.

Mol Cancer Ther 2008;7:2621-2632.